Available online at http://scik.org
Commun. Math. Biol. Neurosci. 2025, 2025:145
https://doi.org/10.28919/cmbn/9578
ISSN: 2052-2541

THE ROLE OF FEAR AND PREDATOR-DEPENDENT REFUGE ON THE DYNAMICS OF THE CARCASSES-PREY-SCAVENGER SYSTEM

DOUAA KHUDHEYER ABID[1], RAID KAMEL NAJI[2,*]
[1]Department of Mathematics, College of Science, University of Baghdad, Baghdad, Iraq
[2]Scientific Research Commission, Baghdad, Iraq

Abstract: A novel ecological model involving carcasses, prey, and scavengers under the influence of fear and predator-dependent refuge is proposed and examined in this research. The main objective of studying such an ecological model is to comprehend the complex trophic interactions and population dynamics within an ecosystem. Beyond simple predator-prey relationships, this type of model takes into account several significant factors that influence the behavior and survival of many species. Since the model is built as a system of nonlinear differential equations, we looked at the existence and stability of equilibria. The prerequisites for persistence were established. The study looked at bifurcation analysis, which shows that altering certain parameters can result in qualitative changes. Furthermore, our obtained results are validated by the use of numerical simulation. The results highlight that the suggested system has only a point attractor and lacks the periodic dynamics typical of a prey-predator system. This indicates that the prey-predator dynamics were stabilized by the presence of carcasses in the habitat.

Keywords: ecological model; predator-dependent refuge; stability; persistence; bifurcation.
2020 AMS Subject Classification: 92D30; 34D20; 34C23.

1. INTRODUCTION

Mathematical models are commonly used to simulate the dynamics of interacting populations. The fundamental prey-predator models developed by Lotka (1925) and Volterra (1926) serve as the foundation for mathematical ecology [1]. Since then, the Lotka-Volterra model paradigm has

*Corresponding author
E-mail address: rknaji@src.edu.iq
Received August 29, 2025

been used to propose and extensively study several mathematical models; see [2-6] and the cited works. These models were extended to incorporate more species and a range of biological characteristics, enabling the production of more realistic simulations. Numerous studies, some involving omnivore species, have constructed food chains or food webs by incorporating a third species into the prey-predator paradigm; see [7–13] and the references therein.

Scavengers are creatures that feed on carrion, which is defined as the remains of animals that have either died naturally or been killed by other species. It's important to keep this in mind. Scavengers are therefore crucial to cleaning up the environment. Few researchers have examined the impact of scavenging in their models, despite the significance of scavengers and the necessity of maintaining their influence on predator-prey dynamics. Nolting et al. [14] examined a three-species system comprising a predator, its prey, and a scavenger. They believed that neither the predator nor its prey was directly impacted by the scavenger species. Even while this assumption seems implausible from a biological standpoint, there are biological circumstances in which this may happen, and it clarified the study. A third predator species that consumed the prey and the predator's carcasses but did not deter the predator population was later incorporated into a predator-prey model developed and investigated by several authors, see [15–18].

To understand how different resources are transported as a trap from one prey-predator system to another, Jansen and Van Gorder [19] created and studied a five-dimensional predator-prey-quarry-resource-scavenger model. This model is an expansion of an already-existing quarry-resource-scavenger model. Predators affect the structure of food webs since it is commonly recognized that they have a detrimental effect on prey biomass and growth efficiency. Fear may be just as effective in lowering prey populations as predation by predators, because it can kill prey and reduce productivity [20–21]. Many prey-predator models have been proposed and examined in detail, where the predator either kills the prey or changes the behavior of the prey population due to fear of predation [22–24]. Later on, Maghool and Naji [25] examined the effects of prey fear and team defense against predation on the dynamics of the food-web model. They discovered that the fear factor leads the predator to extinction after stabilizing the system to a certain extent. Additionally, the quantity and quality of food, with anti-predator behavior, were examined since they have an impact on the system's behavior in relation to the fear element [26-27]. Ibrahim, Bahlool, Satar, and Naji [28] hypothesized and investigated a prey-predator system with a Holling type II functional response, which combines a predator-dependent refuge with predation fear. They discovered that while the system is bistable between a limit cycle and a coexistence equilibrium point, the dread destabilizes the system's dynamics.

In this paper, however, we proposed and analyzed a novel food web model that includes carcasses, prey, and scavengers under the influence of fear and predator-dependent refuge. This model does not negatively affect the predator population because the scavenger is also a predator of the prey and consumes the carcasses of both the prey and the predators that it kills.

The following is the order in which the paper is structured. Section 2 treats the mathematical model formulation with the basic properties of its solution. The conditions of the existence of equilibria and their stability are given in Section 3. Section 4 investigates the persistence of the model. While the global stability is studied in Section 5. Section 6 treats the bifurcation of the system. However, the numerical simulation is the main subject of Section 7. Finally, Section 8 is focused on the main conclusion of the study.

2. FORMULATION OF THE MODEL

In this section, the dynamics of the carcasses-prey-scavenger system under the influence of fear and predator-dependent refuge are formulated mathematically to study. To formulate the dynamics of such a real-life system, the following hypotheses are adopted:

1) Let $C(T)$, $X(T)$, and $Y(T)$ represent the densities at time T for the carcasses (or subsidies for resources), prey, and scavengers, respectively. It's assumed carcasses decay exponentially in the absence of scavengers. However, it is attacked by the scavenger according to the Lotka-Volterra type of functional response.
2) The prey's birth rate is affected due to the prey's fear of the scavenger. Moreover, there is intraspecific competition among individuals of the prey population. Additionally, prey individuals face natural mortality. The environment provides partial protection of prey species against the scavenger with refuge rate $0 < a_2 - b_2 Y < 1$; therefore, there is $a_2 - b_2 Y$ of prey species available for predation.
3) The scavenger species faces a natural death rate. Moreover, the scavenger consumes the carcasses and prey according to the mass action law represented by the Lotka-Volterra type of function response.

Consequently, the dynamics of this model can be represented mathematically with the following set of differential equations:

$$\begin{aligned}\frac{dC}{dT} &= \Lambda - d_1C - a_1CY,\\ \frac{dX}{dT} &= \frac{rX}{1+hY} - d_2X - b_1X^2 - (a_2 - b_2Y)XY,\\ \frac{dY}{dT} &= e_1(a_2 - b_2Y)XY + e_2a_1CY - d_3Y,\end{aligned} \tag{1}$$

with initial conditions, $C(0) > 0$, $X(0) > 0$ and $Y(0) > 0$. While the parameters are described in Table 1.

Table 1: Parameter descriptions

Parameter	Description
$0 < d_1 < 1$	The natural decay rate of carcasses
$a_1 > 0$	The maximum attack rate of carcasses
$r > 0$	The prey's net birth rate
$h \geq 0$	The prey's fear rate
$b_1 > 0$	The intraspecific competition rate of the prey individuals
$0 < d_2 < 1$	The prey's natural death rate
$a_2 > 0$	The maximum attack rate of prey
b_2	The prey's refuge rate
$0 < d_3 < 1$	The scavenger's natural death rate
$0 < e_1 < 1$	The conversion rate from carcasses
$0 < e_2 < 1$	The conversion rate from prey

Now, rewrite the system (1). It becomes:

$$\begin{aligned}\frac{dC}{dT} &= \Lambda - d_1C - a_1CY = f_1(C,X,Y),\\ \frac{dX}{dT} &= X\left[\frac{r}{1+hY} - d_2 - b_1X - (a_2 - b_2Y)Y\right] = Xf_2(C,X,Y),\\ \frac{dY}{dT} &= Y[e_1(a_2 - b_2Y)X + e_2a_1C - d_3] = Yf_3(C,X,Y),\end{aligned} \tag{2}$$

In the following theorem, the positivity and boundedness of the solutions of the system (2) are established.

Theorem 1. All solutions $(C(T), X(T), Y(T))$of the system (2) with initial conditions $C(0) = C_0 > 0$, $X(0) = X_0 > 0$, and $Y(0) = Y_0 > 0$ are positive for all $T > 0$, and uniformly bounded.

Proof: According to equations of system (2), together with the given initial conditions, it is obtained:

$$C(T) > C_0exp(-\int_0^T (d_1 + a_1Y(s))ds > 0\,,$$

$$X(T) = X_0exp\left(\int_0^T f_2\big(C(T), X(S), Y(s)\big)ds\right) > 0\,,$$

$$Y(T) = Y_0 exp\left(\int_0^T f_3\big(C(T), X(S), Y(s)\big)ds\right) > 0.$$

Hence, all solutions starting from the interior of the first octant remain in it for all future time. From the first equation, it is observed that

$$\frac{dC}{dT} \leq \Lambda - d_1 C.$$

Now, according to Lemma 2.1 [29], it is obtained that:

$$C(T) \leq \frac{\Lambda}{d_1}\left[1 + \left(\frac{d_1}{\Lambda}C_0 - 1\right)e^{-d_1 T}\right].$$

Hence, as $T \to \infty$, then $C(T) \leq \frac{\Lambda}{d_1}$.

From the second equation, it was observed that

$$\frac{dX}{dT} \leq \frac{rX}{1+hY} - d_2 X - b_1 X^2 \leq X(r - d_2 - b_1 X) \leq (r - d_2)X\left(1 - \frac{1}{\frac{r-d_2}{b_1}}X\right).$$

Then, according to Lemma 2.2 [29], it is obtained that:

$$X(T) \leq \frac{r-d_2}{b_1}\left[1 + \left(\frac{r-d_2}{b_1}{X_0}^{-1} - 1\right)e^{-(r-d_2)T}\right]^{-1}.$$

Then, for $T \to \infty$, then $X(T) \leq \frac{r-d_2}{b_1}$.

Let us consider $\zeta(T) = \frac{e_2}{e_1}C + X(T) + \frac{1}{e_1}Y(T)$. Then the derivative along time of the solution of system (2) is given by

$$\frac{d\zeta(T)}{dT} = \frac{e_2}{e_1}\Lambda - \frac{e_2}{e_1}d_1 C + \frac{rX}{1+hY} - d_2 X - b_1 X^2 - \frac{1}{e_1}d_3 Y.$$

Therefore, it's obtained that:

$$\frac{d\zeta(T)}{dT} \leq \frac{e_2}{e_1}\Lambda - \frac{e_2}{e_1}d_1 C + rX - d_2 X - \frac{1}{e_1}d_3 Y.$$

$$\leq \frac{e_2}{e_1}\Lambda + r\left(\frac{r-d_2}{b_1}\right) - \mu\left(\frac{e_2}{e_1}C + X + \frac{1}{e_1}Y\right) = \Lambda_1 - \mu\zeta(T),$$

where $\mu = min\,\{d_1, d_2, d_3\}$. Again, according to Lemma 2.1 [29], it is obtained that:

$$\zeta(T) \leq \frac{\Lambda_1}{\mu}\left[1 + \left(\frac{\mu}{\Lambda_1}\zeta(0) - 1\right)e^{-\mu T}\right].$$

Hence, as $T \to \infty$, then $\zeta(T) \leq \frac{\Lambda_1}{\mu}$. Thus, the proof is complete.

3. EXISTENCE AND STABILITY OF EQUILIBRIA

To comprehend how ecosystems react to minor disturbances near their equilibrium states, it is essential to study local stability analysis in ecological systems. Ecologists and mathematicians can use this methodology to forecast whether a system will diverge and possibly cause severe changes like population collapse or ecosystem upheavals, or whether it will return to equilibrium after a small shock. There are at most four nonnegative equilibrium points of the system (2). The existing conditions and stability analyses of them are described below:

The axial equilibrium point $P_C = \left(\frac{\Lambda}{d_1}, 0,0\right)$ of system (2) exists irrespective of any parametric restriction:

The first boundary equilibrium point in CX −plane is given by $P_{CX} = (\bar{C}, \bar{X}, 0) = \left(\frac{\Lambda}{d_1}, \frac{r-d_2}{b_1}, 0\right)$, which is feasible under the condition:

$$r > d_2. \tag{3}$$

The second boundary equilibrium point in $CY-$ plane is given by $P_{CY} = (\hat{C}, 0, \hat{Y}) = \left(\frac{d_3}{e_2 a_1}, 0, \frac{e_2 \Lambda a_1 - d_1 d_3}{a_1 d_3}\right)$, which exists under the parametric restriction:

$$e_2 \Lambda a_1 > d_1 d_3. \tag{4}$$

There is a unique interior equilibrium point $P_* = (C_*, X_*, Y_*)$ where

$$\left.\begin{aligned} C_* &= \frac{\Lambda}{d_1 + a_1 Y_*} \\ X_* &= \frac{r - d_2(1+hY_*) - (a_2 - b_2 Y_*)Y_*(1+hY_*)}{b_1(1+hY_*)} \end{aligned}\right\}. \tag{5}$$

With Y_* being a positive root of the fifth-order equation:

$$\beta_1 Y^5 + \beta_2 Y^4 + \beta_3 Y^3 + \beta_4 Y^2 + \beta_5 Y^1 + \beta_6 = 0,$$

where:

$$\beta_1 = e_1 b_2^2 a_1 h > 0.$$

$$\beta_2 = -2h a_1 a_2 b_2 e_1 + a_1 b_2^2 e_1 + h b_2^2 d_1 e_1.$$

$$\beta_3 = h a_1 a_2^2 e_1 - 2a_1 a_2 b_2 e_1 - 2h a_2 b_2 d_1 e_1 + b_2^2 d_1 e_1 - h a_1 b_2 d_2 e_1.$$

$$\begin{aligned} \beta_4 = {} & h a_1 b_1 d_3 + a_1 a_2^2 e_1 + r a_1 b_2 e_1 + h a_2^2 d_1 e_1 - 2a_2 b_2 d_1 e_1 \\ & + h a_1 a_2 d_2 e_1 - a_1 b_2 d_2 e_1 - h b_2 d_1 d_2 e_1 \end{aligned}.$$

$$\begin{aligned} \beta_5 = {} & a_1 b_1 d_3 + h b_1 d_1 d_3 - r a_1 a_2 e_1 + a_2^2 d_1 e_1 + r b_2 d_1 e_1 + a_1 a_2 d_2 e_1 \\ & + h a_2 d_1 d_2 e_1 - b_2 d_1 d_2 e_1 - h \Lambda a_1 b_1 e_2 \end{aligned}.$$

$$\beta_6 = -r a_2 d_1 e_1 - \Lambda a_1 b_1 e_2 + a_2 d_1 d_2 e_1 + b_1 d_1 d_3.$$

Accordingly, P_* exists uniquely in the interior of the positive octant $int.\mathbb{R}_+^3$ provided that the following sufficient conditions are met.

$$[d_2 + (a_2 - b_2 Y_*) Y_*](1 + hY_*) < r. \tag{6}$$

With one set of the following conditions:

$$\left.\begin{array}{l} \beta_2 > 0\,, \beta_3 > 0, \beta_4 > 0\,, \beta_5 > 0\,, \beta_6 < 0 \\ \beta_2 < 0\,, \beta_3 < 0, \beta_4 < 0\,, \beta_5 < 0\,, \beta_6 < 0 \\ \beta_2 > 0\,, \beta_3 > 0, \beta_4 < 0\,, \beta_5 < 0\,, \beta_6 < 0 \\ \beta_2 > 0\,, \beta_3 > 0, \beta_4 > 0\,, \beta_5 < 0\,, \beta_6 < 0 \\ \beta_2 > 0\,, \beta_3 > 0, \beta_4 > 0\,, \beta_5 < 0\,, \beta_6 < 0 \end{array}\right\} \tag{7}$$

For the stability analysis of the above equilibrium points, consider the Jacobian matrix M at point (C, X, Y) that can be written as:

$$M(C, X, Y) = \begin{bmatrix} \frac{\partial f_1}{\partial C} & \frac{\partial f_1}{\partial X} & \frac{\partial f_1}{\partial Y} \\ X\frac{\partial f_2}{\partial C} & X\frac{\partial f_2}{\partial X} + f_2 & X\frac{\partial f_2}{\partial Y} \\ Y\frac{\partial f_3}{\partial C} & Y\frac{\partial f_3}{\partial X} & Y\frac{\partial f_3}{\partial Y} + f_3 \end{bmatrix}, \tag{8}$$

where:

$$\frac{\partial f_1}{\partial C} = -d_1 - a_1 Y,\ \frac{\partial f_1}{\partial X} = 0,\ \frac{\partial f_1}{\partial Y} = -a_1 C,$$

$$\frac{\partial f_2}{\partial C} = 0,\ \frac{\partial f_2}{\partial X} = -b_1,\ \frac{\partial f_2}{\partial Y} = \frac{-rh}{(1+hy)^2} - a_2 + 2b_2 Y,$$

$$\frac{\partial f_3}{\partial C} = e_2 a_1,\ \frac{\partial f_3}{\partial X} = e_1(a_2 - b_2 Y),\ \ \frac{\partial f_3}{\partial Y} = -e_1 b_2 X.$$

Now, by substituting the above equilibrium points in $M(C, X, Y)$, and then computing their eigenvalues, it is observed that:

At the axial equilibrium point $P_C = (\frac{\Lambda}{d_1}, 0,0)$, the eigenvalues of $M(P_C)$ are given by $\lambda_{11} = -d_1$, $\lambda_{12} = r - d_2$, and $\lambda_{13} = \frac{e_2 a_1 \Lambda - d_3 d_1}{d_1}$. Thus, the axial equilibrium point P_1 is locally asymptotically stable if the following set of conditions holds.

$$\left.\begin{array}{c} r < d_2 \\ e_2 a_1 \Lambda < d_3 d_1 \end{array}\right\}. \tag{9}$$

Moreover, the axial equilibrium point P_C loses its stability when at least one of the above conditions is violated, and it becomes a saddle node.

At the first boundary equilibrium point $P_{CX} = (\bar{C}, \bar{X}, 0) = \left(\frac{\Lambda}{d_1}, \frac{r-d_2}{b_1}, 0\right)$. The eigenvalues of $M(P_{CX})$ are given by $\lambda_{21} = -d_1 < 0$, $\lambda_{22} = d_2 - r < 0$, and $\lambda_{23} = \frac{e_2 a_1 \Lambda b_1 + d_1 e_1 a_2 (r - d_2) - d_3 d_1 b_1}{d_1 b_1}$. Then, the first boundary equilibrium point P_{CX} is locally asymptotically stable if the condition

$$e_2 a_1 \Lambda b_1 + d_1 e_1 a_2 (r - d_2) < d_3 d_1 b_1. \tag{10}$$

The first boundary equilibrium point loses its stability when the above conditions are violated, and it becomes a saddle node.

At the second boundary equilibrium point $P_{CY} = (\hat{C}, 0, \hat{Y}) = \left(\frac{d_3}{e_2 a_1}, 0, \frac{e_2 \Lambda a_1 - d_1 d_3}{a_1 d_3}\right)$, the eigenvalues of $M(P_{CY})$ are given by:

$$\lambda_{31}, \lambda_{33} = \frac{-(d_1 + a_1 \hat{Y}) \pm \sqrt{(d_1 + a_1 \hat{Y})^2 - 4 a_1{}^2 e_2 \hat{Y} \hat{C}}}{2},$$
$$\lambda_{32} = \frac{r}{1 + h\hat{Y}} - d_2 - (a_2 - b_2 \hat{Y})\hat{Y}.$$

The second boundary equilibrium point is locally asymptotically stable if the following condition holds:

$$r < [d_2 + (a_2 - b_2 \hat{Y})\hat{Y}](1 + h\hat{Y}). \tag{11}$$

Otherwise, it is unstable.

Finally, for the interior equilibrium point $P_* = (C_*, X_*, Y_*)$, the Jacobian matrix can be written

$$M(P_*) = \begin{bmatrix} -d_1 - a_1 Y_* & 0 & -a_1 C_* \\ 0 & -b_1 X^* & X_* \left(\frac{-rh}{(1+hY_*)^2} - a_2 + 2 b_2 Y_*\right) \\ e_2 a_1 Y_* & Y_* (e_1 (a_2 - b_2 Y_*)) & -e_1 b_2 X_* Y_* \end{bmatrix} = [a_{ij}]. \tag{12}$$

The characteristic equation associated with $M(P_*)$ is given by:

$$\lambda^3 + A_1 \lambda^2 + A_2 \lambda + K = 0, \tag{13}$$

where:

$$A_1 = -(a_{11} + a_{22} + a_{33}).$$
$$A_2 = a_{11} a_{22} + a_{11} a_{33} + a_{22} a_{33} - a_{23} a_{32} - a_{13} a_{31}.$$
$$K = -(a_{11} a_{22} a_{33} - a_{11} a_{23} a_{32} - a_{13} a_{31} a_{22}).$$

With:

$$\begin{aligned} \Delta = A_1 A_2 - K = -a_{11} a_{22} (a_{11} + a_{22}) - (a_{11} + a_{33})[a_{11} a_{33} - a_{13} a_{31}] \\ -(a_{22} + a_{33})[a_{22} a_{33} - a_{23} a_{32}] - 2 a_{11} a_{22} a_{33} \end{aligned}.$$

Consequently, the local stability of the coexistence equilibrium point of system (2) can be discussed in the following theorem.

Theorem 2. The coexistence equilibrium point of system (2) is locally stable in the interior of $\mathbb{R}^3_+$ provided that the following sufficient condition holds.

$$2 b_2 Y_* < \frac{rh}{(1+hY_*)^2} + a_2. \tag{14}$$

Proof. According to the Routh-Hurwitz criterion, equation (13) has three roots with negative real parts provided that $A_1 > 0$, $K > 0$, and $\Delta > 0$.

Direct computation shows that all requirements of the Routh-Hurwitz criterion are satisfied under the sufficient condition (14). Hence, all the eigenvalues of $M\ (P_*)$ have negative real parts, and therefore the proof follows. This implies P_* is locally asymptotically stable.

4. PERSISTENCE

Understanding how ecosystems sustain their structure, function, and biodiversity over time, despite disturbances and environmental changes, requires an understanding of persistence in ecological systems. Accordingly, two subsystems can be driven from the system (2). These are written as follows:

First Subsystem, which belongs to CX −Plane, is written as:

$$\left.\begin{aligned} \frac{dC}{dT} &= \Lambda - d_1 C = f_1(C,X,Y) = h_1(C,X) \\ \frac{dX}{dT} &= X(r - d_2 - b_1 X) = h_2(C,X) \end{aligned}\right\}. \tag{15}$$

While the second subsystem, which is in the CY −Plane, is written as:

$$\left.\begin{aligned} \frac{dC}{dT} &= \Lambda - d_1 C - a_1 CY = g_1(C,Y) \\ \frac{dY}{dT} &= Y(e_2 a_1 C - d_3) = g_2(C,Y) \end{aligned}\right\}. \tag{16}$$

Consider the Dulac functions given by $B_1(C,X) = \frac{1}{X}$ and $B_2(C,Y) = \frac{1}{Y}$, which satisfy $B_i > 0$, $i = 1,2$ and C' function in the int. $\mathbb{R}_+^2$ of $CX-$ and CY −planes respectively.

Hence, direct computation shows that:

$$\Delta(C,X) = \frac{\partial B_1 h_1}{\partial C} + \frac{\partial B_1 h_2}{\partial X} = -\frac{d_1}{X} - \mathrm{b}_1 < 0.$$

$$\Delta(C,Y) = \frac{\partial B_2 g_1}{\partial C} + \frac{\partial B_2 g_2}{\partial X} = -\frac{d_1}{Y} - \mathrm{a}_1 < 0.$$

Then $\Delta(C,X)$ and $\Delta(C,Y)$ do not identify zero in the int. $\mathbb{R}_+^2$ of their planes and does not change the sign.

Thus, there is no closed cure in the $int.\mathbb{R}_+^2$ of the $CX-$ and CY −planes according to Dulac-Bendixson criterion [30]. Furthermore, the Pioncare-Bendixson theorem [30] states that the unique equilibrium point in the $int.\mathbb{R}_+^2$ of the $CX-$ and CY −planes, as defined by P_{CX} and P_{CY}, are globally asymptotically stable whenever they are locally stable.

Theorem 3: The system (2) is uniformly persistent if the following requirements are met:

$$\left.\begin{array}{c} d_2 < r \\ or \\ d_3 d_1 < e_2 a_1 \Lambda \end{array}\right\} . \tag{17}$$

$$d_3 < e_1 a_2 \bar{X} + e_2 a_1 \bar{C}. \tag{18}$$

$$\left[d_2 + \left(a_2 - b_2 \hat{Y}\right)\hat{Y}\right]\left(1 + h\hat{Y}\right) < r. \tag{19}$$

Proof: According to the method of average Lyapunov function [31], define the function $\varphi(C,X,Y) = C^{q_1} X^{q_2} Y^{q_3}$, where $q_i, \forall i = 1,2,3$ are positive constants. Hence, for all $(C,X,Y)) \in int.\mathbb{R}^3_+$, then $\varphi(C,X,Y) \to 0$, when any one of their variables approaches zero. Furthermore, it is obtained that

$$\Omega(C,X,Y) = \frac{\varphi'(C,X,Y)}{\varphi(C,X,Y)} = \frac{q_1}{C} f_1 + q_2 f_2 + q_3 f_3.$$

Now, since there are no periodic attractors in the boundary planes, the only possible omega limit sets of system (2) are the equilibrium points P_C, P_{CX}, and P_{CY}. Thus, the system is uniformly persistent if we can prove $\Omega(.) > 0$ at each of these points. Also we have

$$\Omega(P_C) = q_2(r - d_2) + q_3\left(e_2 a_1 \frac{\Lambda}{d_1} - d_3\right).$$

$$\Omega(P_{CX}) = q_3(e_1 a_2 \bar{X} + e_2 a_1 \bar{C} - d_3).$$

$$\Omega(P_{CY}) = q_2\left(\frac{r}{1+h\hat{Y}} - d_2 - \left(a_2 - b_2\hat{Y}\right)\hat{Y}\right).$$

Obviously, $\Omega(P_C) > 0$ for a suitable choice of positive constants $q_i, i = 2,3$ provided that the conditions (17) are satisfied. However, $\Omega(P_{CX})$ and $\Omega(P_{CY})$ are positive provided that the conditions (18) and (19) are satisfied, respectively. Then the system (2) is uniformly persistent.

5. GLOBAL STABILITY

Gaining a thorough grasp of ecological systems' long-term behavior and resilience is the goal of studying their global stability. This knowledge is essential for tackling urgent environmental issues and guaranteeing the sustainability of our planet's ecosystems. Therefore, this section treats the global stability of the system (2).

Theorem 4: Suppose that $P_C = \left(\frac{\Lambda}{d_1}, 0, 0\right)$ is locally asymptotically stable, then it is globally asymptotically stable, provided that:

$$\frac{a_1 \Lambda}{d_1} < d_3. \tag{20}$$

Proof: Define the real valued function $\mho_1 = \left(C - C_0 - C_0 \ln\frac{C}{C_0}\right) + X + Y$, with $C_0 = \frac{\Lambda}{d_1}$. Direct computation shows that $\mho_1 : U_1 \to \mathbb{R}$, where $U_1 = \{(C,X,Y) \in \mathbb{R}^3_+, C > 0, X \geq 0, Y \geq 0\}$, so that

$\mho_1(P_C) = 0$ and $\mho_1(C, X, Y) > 0, \forall\, (C, X, Y) \in U_1 - P_C$. Moreover, straightforward computation gives that:

$$\frac{d\mho_1}{dT} = \left(\frac{C - C_0}{C}\right)\frac{dC}{dT} + \frac{dX}{dT} + \frac{dY}{dT} \le -\frac{d_1}{C}(C - C_0)^2 - (d_3 - a_1 C_0)Y - (d_2 - r)X.$$

Hence, under the local stability condition (9) with the condition (20) given that $\frac{d\mho_1}{dT} < 0$.

Hence, P_C is globally asymptotically stable.

Theorem 5: The first boundary equilibrium point $P_{CX} = \left(\frac{\Lambda}{d_1}, \frac{r - d_2}{b_1}, 0\right)$ is globally asymptotically stable, if the following condition holds:

$$a_1\bar{C} + (rh + a_2)\bar{X} < d_3. \tag{21}$$

Proof: Define the real valued function $\mho_2 = \left(C - \bar{C} - \bar{C}\, ln\frac{C}{\bar{C}}\right) + (X - \bar{X} - \bar{X} ln\frac{X}{\bar{X}}) + Y$, with $\bar{C} = \frac{\Lambda}{d_1}$ and $\bar{X} = \frac{r - d_2}{b_1}$. Direct computation shows that $\mho_2\colon U_2 \to \mathbb{R}$ where $U_2 = \{(C, X, Y) \in \mathcal{R}_+^3, C > 0, X > 0, Y \ge 0\,\}$, so that $\mho_2(P_{CX}) = 0$ and $\mho_2(C, X, Y) > 0, \forall\, (C, X, Y) \in U_2 - P_{CX}$. Moreover, straightforward computation gives that

$$\frac{d\mho_2}{dT} \le -\frac{d_1}{C}(C - \bar{C})^2 - b_1(X - \bar{X})^2 - [d_3 - a_1\bar{C} + (rh + a_2)\bar{X}]Y.$$

Hence, condition (21) yields $\frac{d\mho_2}{dT} < 0$. Hence, P_{CX} is globally asymptotically stable.

Theorem 6: The second boundary equilibrium point $P_{CY} = \left(\frac{d_3}{a_1 e_2}, 0, \frac{e_2 a_1 \Lambda - d_3 d_1}{a_1 d_3}\right)$ is globally asymptotically stable, if the following condition holds:

$$r < d_2. \tag{22}$$

Proof: Define the real valued function $\mho_3 = n_1 \frac{1}{2}\left(C - \hat{C}\right)^2 + n_2 X + n_3\left(Y - \hat{Y} - \hat{Y}\ln\frac{Y}{\hat{Y}}\right)$, with $\hat{C} = \frac{d_3}{a_1 e_2}$, $\hat{Y} = \frac{e_2 a_1 \Lambda - d_3 d_1}{a_1 d_3}$, and $n_i, i = 1{,}2{,}3$ are positive constants. Direct computation shows that $\mho_3\colon U_3 \to \mathbb{R}$, where $U_3 = \{(C, X, Y) \in \mathbb{R}_+^3, C \ge 0, X \ge 0, Y > 0\,\}$, so that $\mho_3(P_{CY}) = 0$ and $\mho_3(C, X, Y) > 0, \forall\, (C, X, Y) \in U_3 - P_{CY}$. Moreover, straightforward computation gives that:

$$\frac{d\mho_3}{dT} = n_1\left(C - \hat{C}\right).\frac{dC}{dT} + n_2\frac{dX}{dT} + n_3\frac{(Y - \hat{Y})}{Y}\frac{dY}{dT}.$$

Therefore, it is obtained that:

$$\begin{gathered}\frac{d\mho_3}{dT} = -n_1(d_1 + a_1 Y)\left(C - \hat{C}\right)^2 - n_1 a_1\hat{C}\left(C - \hat{C}\right)\left(Y - \hat{Y}\right) + n_2\frac{rX}{1 + hY} \\ -n_2 d_2 X - n_2 b_1 X^2 - n_2(a_2 - b_2 Y)YX + n_3 e_1(a_2 - b_2 Y)XY \\ -n_3 e_1(a_2 - b_2 Y)X\hat{Y} + n_3 e_2 a_1\left(C - \hat{C}\right)\left(Y - \hat{Y}\right)\end{gathered}.$$

Then choosing the constants as $n_1 = \frac{e_2}{\hat{C}}$, $n_2 = e_1$, and $n_3 = 1$, yield that:

$$\frac{d\mho_3}{dT} \leq -\frac{e_2}{\hat{C}}(d_1 + a_1 Y)\left(C - \hat{C}\right)^2 - e_1(d_2 - r)X.$$

According to condition (22), $\frac{d\mho_3}{dT}$ is negative semidefinite.

Furthermore, the P_{CY} turns into an attractive point using LaSalle's invariance principle because the singleton set $\{P_{CY}\}$ is the only invariant set that belongs to the set of points that makes $\frac{d\mho_3}{dT} = 0$. The second boundary equilibrium point is hence globally asymptotically stable.

Theorem 7: The interior equilibrium point P_* is globally asymptotically stable if the following conditions hold: (C_*, X_*, Y_*)

$$\frac{1}{2}[rhe_1 - e_1 b_2 Y_*]^2 < e_1 b_1. \tag{23}$$

$$\frac{1}{2} < e_1 b_2 X_*. \tag{24}$$

Proof: Define the real valued function $\mho_4 = n_4 \frac{1}{2}(C - C_*)^2 + n_5\left(X - X_* - X_* ln\frac{X}{X_*}\right) + n_6\left(Y - Y_* - Y_* ln\frac{Y}{Y_*}\right)$, with $n_i, i = 4,5,6$ are positive constants. Direct computation shows that $\mho_4 : U_4 \to \mathbb{R}$, where $U_4 = \{(C, X, Y) \in \mathbb{R}^3_+, C \geq 0, X > 0, Y > 0\}$, so that $\mho_4(P_*) = 0$ and $\mho_4(C, X, Y) > 0, \forall\ (C, X, Y) \in U_4 - P_*$. Moreover, straightforward computation gives that:

$$\frac{d\mho_4}{dT} = n_4(C - C_*).\frac{dC}{dT} + n_5\frac{(X - X_*)}{X}\frac{dX}{dT} + n_6\frac{(Y - Y_*)}{Y}\frac{dY}{dT}.$$

Therefore, it is obtained that:

$$\begin{aligned}\frac{d\mho_4}{dT} &= -n_4(d_1 + a_1 Y)(C - C_*)^2 - [n_4 a_1 C_* - n_6 e_2 a_1](C - C_*)(Y - Y_*) \\ &\quad - \frac{rhn_5(X - X_*)(Y - Y_*)}{1 + hY} - n_5 b_1 (X - X_*)^2 - n_6 e_1 b_2 X_* (Y - Y_*)^2 \\ &\quad + [n_6 e_1 a_2 - n_6 e_1 b_2 Y + n_5 b_2 (Y + Y_*) - n_5 a_2](X - X_*)(Y - Y_*)\end{aligned}.$$

Then choosing the constants as $n_4 = \frac{e_2}{C_*}$, $n_5 = e_1$, and $n_6 = 1$, yield that:

$$\begin{aligned}\frac{d\mho_4}{dT} \leq -\frac{e_2}{C_*}(d_1 + a_1 Y)(C - C_*)^2 - \left(e_1 b_1 - \frac{1}{2}\left[\frac{rhe_1}{1 + hY} - e_1 b_2 Y_*\right]^2\right)(X - X_*)^2 \\ - \left(e_1 b_2 X_* - \frac{1}{2}\right)(Y - Y_*)^2\end{aligned}$$

Therefore, conditions (23) and (24) yield $\frac{d\mho_4}{dT} < 0$. Hence, P_* is globally asymptotically stable.

6. LOCAL BIFURCATION ANALYSIS

Better-informed judgments in ecology, conservation, and resource management are ensured by the mathematical toolkit that local bifurcation analysis offers to predict and control sudden ecological changes. Ecologists can anticipate when and why systems may experience significant shifts by researching bifurcations, which helps avert unfavorable events like extinctions or ecological collapses. Therefore, in this section, the occurrence of local bifurcation in system (2) is investigated. Note that system (2) should be rewritten as $\frac{dX}{dT} = F(X)$, where $X = (C, X, Y)^T$ and $F(X) = (f_1, Xf_2, Yf_3)^T$.

The second directional derivative of the general Jacobian matrix can be represented as follows:

$$D^2F(\boldsymbol{v}, \boldsymbol{v}) = [c_{i1}]_{3\times1}, \tag{25}$$

where $\boldsymbol{v} = (v_1, v_2, v_3)^T$ be a vector with:

$$c_{11} = -2a_1v_1v_3.$$

$$c_{21} = -2b_1v_2^2 + 2\left(\frac{rh^2X}{(1+hY)^3} + b_2X\right)v_3^2 - 2\left(\frac{rh}{(1+hY)^2} + a_2 - 2b_2Y\right)v_2v_3.$$

$$c_{31} = 2e_2a_1v_1v_3 - 2e_1b_2Xv_3^2 + 2(e_1a_2 - 2e_1b_2Y)v_2v_3.$$

While the third directional derivative of the general Jacobian matrix can be represented as follows:

$$D^3F(\boldsymbol{v}, \boldsymbol{v}, \boldsymbol{v}) = [k_{i1}]_{3\times1}, \tag{26}$$

where:

$$k_{11} = 0.$$

$$k_{21} = \frac{6(1+hY)(h^2r+(1+hY)^3b_2)v_2v_3^2 - 6h^3rXv_3^3}{(1+hY)^4}.$$

$$k_{31} = -6b_2e_1v_2v_3^2.$$

Theorem 8: System (2) exhibits a transcritical bifurcation around $P_c = (\frac{\Lambda}{d_1}, 0, 0)$, when the parameter d_3 passes through the value $\frac{e_2a_1\Lambda}{d_1} = \tilde{d}_3$ with $r \neq d_2$.

Proof. The Jacobian matrix of the system (2) at P_c with $d_3 = \tilde{d}_3$, can be written in the form:

$$M(P_c, \tilde{d}_3) = \begin{bmatrix} -d_1 & 0 & -\frac{a_1\Lambda}{d_1} \\ 0 & r - d_2 & 0 \\ 0 & 0 & 0 \end{bmatrix}.$$

Hence, the eigenvalues of $M(P_c, \tilde{d}_3)$ are given by $\lambda_{11} = -d_1 < 0$, $\lambda_{12} = r - d_2$, and $\lambda_{13} = 0$. Let $\tilde{\boldsymbol{v}} = (v_{11}, v_{12}, v_{13})^T$, and $\tilde{\boldsymbol{\psi}} = (\psi_{11}, \psi_{12}, \psi_{13})^T$ be the eigenvectors of $M(P_c, \tilde{d}_3)$, and $\left[M(P_c, \tilde{d}_3)\right]^T$ associated with $\lambda_{13} = 0$, then it obtain that $\tilde{\boldsymbol{v}} = (-\frac{a_1\Lambda}{d_1^2}, 0, 1)^T$, and $\tilde{\boldsymbol{\psi}} = (0,0,1)^T$. Moreover, direct computation using Eq. (25) shows that:

$$\frac{\partial F}{\partial d_3} = F_{d_3} = (0,0,-Y)^T \Rightarrow \tilde{\boldsymbol{\psi}}^T[F_{d_3}(P_c, \tilde{d}_3)] = 0.$$

$$\tilde{\boldsymbol{\psi}}^T[DF_{d_3}(P_c, \tilde{d}_3)\tilde{\boldsymbol{v}}] = -1.$$

$$\tilde{\boldsymbol{\psi}}^T[D^2F(P_c, \tilde{d}_3)(\tilde{\boldsymbol{v}}, \tilde{\boldsymbol{v}})] = -2e_2\frac{a_1^2\Lambda}{d_1^2}.$$

Hence, there is a transcritical bifurcation in the sense of Sotomayer's theorem [30].

Theorem 9: System (2) exhibits a transcritical bifurcation around $P_{CX} = \left(\frac{\Lambda}{d_1}, \frac{r-d_2}{b_1}, 0\right)$, when the parameter e_2 passes through the positive value $\bar{e}_2 = \frac{b_1 d_1 d_3 - e_1 a_2 d_1 (r-d_2)}{a_1 b_1 \Lambda}$.

Proof. The Jacobian matrix of the system (2) at P_{CX} with $e_2 = \bar{e}_2$ can be written in the form:

$$M(P_{CX}, \bar{e}_2) = \begin{bmatrix} -d_1 & 0 & -a_1 \frac{\Lambda}{d_1} \\ 0 & -(r-d_2) & -\frac{(rh+a_2)(r-d_2)}{b_1} \\ 0 & 0 & 0 \end{bmatrix}.$$

Hence, the eigenvalues of $M(P_{CX}, \bar{e}_2)$ are given by $\bar{\lambda}_{21} = -d_1$, $\bar{\lambda}_{22} = -(r-d_2)$, and $\bar{\lambda}_{23} = 0$. Let $\bar{\boldsymbol{v}} = (\bar{v}_{21}, \bar{v}_{22}, \bar{v}_{23})^T$, and $\bar{\boldsymbol{\psi}} = (\bar{\psi}_{21}, \bar{\psi}_{22}, \bar{\psi}_{23})^T$ be the eigenvectors of $M(P_{CX}, \bar{\Lambda})$, and $[M(P_{CX}, \bar{e}_2)]^T$ associated with $\bar{\lambda}_{23} = 0$, then it obtain that $\bar{\boldsymbol{v}} = \left(-\frac{a_1 \Lambda}{d_1^2}, -\frac{(rh+a_2)}{b_1}, 1\right)^T$, and $\bar{\boldsymbol{\psi}} = (0,0,1)^T$.

Moreover, direct computation using Eq. (25) shows that:

$$\frac{\partial F}{\partial e_2} = F_{e_2} = (0,0, a_1 CY)^T \Rightarrow \bar{\boldsymbol{\psi}}^T [F_{e_2}(P_{CX}, \bar{e}_2)] = 0.$$

$$\bar{\boldsymbol{\psi}}^T [DF_{e_2}(P_{CX}, \bar{e}_2)\bar{\boldsymbol{v}}] = \frac{a_1 \Lambda}{d_1}.$$

$$\bar{\boldsymbol{\psi}}^T [D^2 F(P_{CX}, \bar{e}_2)(\bar{\boldsymbol{v}}, \bar{\boldsymbol{v}})] = -2\bar{e}_2 \frac{a_1^2 \Lambda}{d_1^2} - 2e_1 b_2 \left(\frac{r-d_2}{b_1}\right) - 2e_1 a_2 \frac{(rh+a_2)}{b_1} \neq 0.$$

Hence, there is a transcritical bifurcation in the sense of Sotomayor's theorem.

Theorem 10: System (2) exhibits a transcritical bifurcation around $P_{CY} = (\hat{C}, 0, \hat{Y})$, when the parameter r passes through the value $\hat{r} = \left[d_2 + \left(a_2 - b_2 \hat{Y}\right)\hat{Y}\right]\left(1 + h\hat{Y}\right)$, provided that the following condition holds:

$$-2b_1 - 2\left(\frac{rh}{(1+h\hat{Y})^2} + a_2 - 2b_2\hat{Y}\right)\left(\frac{e_1(a_2 - b_2\hat{Y})(d_1 + a_1\hat{Y})}{e_2 a_1^2 \hat{C}}\right) \neq 0. \tag{27}$$

Otherwise, a pitchfork bifurcation takes place.

Proof. The Jacobian matrix of the system (2) at P_{CY} with $r = \hat{r}$ can be written in the form:

$$M(P_{CY}, \hat{r}) = \begin{bmatrix} -d_1 - a_1\hat{Y} & 0 & -a_1\hat{C} \\ 0 & 0 & 0 \\ e_2 a_1 \hat{Y} & e_1\left(a_2 - b_2\hat{Y}\right)\hat{Y} & 0 \end{bmatrix}.$$

Hence, the eigenvalues of $M(P_{CY}, \hat{r})$ are given by $\hat{\lambda}_{31}, \hat{\lambda}_{33} = \frac{-(d_1+a_1\hat{Y}) \pm \sqrt{(d_1+a_1\hat{Y})^2 - 4{a_1}^2 e_2 \hat{Y}\hat{C}}}{2}$, and $\hat{\lambda}_{32} = 0$.

Let $\hat{\boldsymbol{v}} = (\hat{v}_{31}, \hat{v}_{32}, \hat{v}_{33})^T$, and $\hat{\boldsymbol{\psi}} = (\hat{\psi}_{31}, \hat{\psi}_{32}, \hat{\psi}_{33})^T$ be the eigenvectors of $M(P_{CY}, \hat{r})$, and

$[M(P_{CY},\hat{r})]^T$ associated with $\hat{\lambda}_{32}=0$, then it obtain that $\hat{\boldsymbol{v}}=\left(-\frac{e_1(a_2-b_2\hat{Y})}{e_2a_1},1,\frac{e_1(a_2-b_2\hat{Y})(d_1+a_1\hat{Y})}{e_2a_1^2\hat{C}}\right)^T$, and $\hat{\boldsymbol{\psi}}=(0,1,0)^T$.

Moreover, direct computation using Eq. (25) shows that:

$$\frac{\partial F}{\partial r}=F_r=\left(0,\frac{X}{1+hY},0\right)^T \Rightarrow \hat{\boldsymbol{\psi}}^T[F_r(P_{CY},\hat{r})]=0.$$

$$\hat{\boldsymbol{\psi}}^T[DF_r(P_{CY},\hat{r})\hat{\boldsymbol{v}}]=\frac{1}{1+h\hat{Y}}.$$

$$\hat{\boldsymbol{\psi}}^T[D^2F(P_{CY},\hat{r})(\hat{\boldsymbol{v}},\hat{\boldsymbol{v}})]=-2b_1-2\left(\frac{rh}{(1+h\hat{Y})^2}+a_2-2b_2\hat{Y}\right)\left(\frac{e_1(a_2-b_2\hat{Y})(d_1+a_1\hat{Y})}{e_2a_1^2\hat{C}}\right).$$

Hence, under the condition (27), there is a transcritical bifurcation in the sense of Sotomayor's theorem.

Otherwise, an application to Eq. (26) shows that:

$$\hat{\boldsymbol{\psi}}^T[D^3F(P_{CY},\hat{r})(\hat{\boldsymbol{v}},\hat{\boldsymbol{v}},\hat{\boldsymbol{v}})]=\frac{6(h^2r+(1+h\hat{Y})^3b_2)}{(1+h\hat{Y})^3}\left(\frac{e_1(a_2-b_2\hat{Y})(d_1+a_1\hat{Y})}{e_2a_1^2\hat{C}}\right)^2\neq 0.$$

Hence, there is a pitchfork bifurcation in the sense of Sotomayor's theorem.

Theorem 11: System (2) undergoes a saddle-node bifurcation near the interior equilibrium point P_* when the parameter b_1 passes through the value $b_1^*=\frac{a_{11}a_{23}a_{32}}{(-a_{11}a_{33}+a_{13}a_{31})X^*}$, provided that the following conditions:

$$2b_2Y_*>\frac{rh}{(1+hY_*)^2}+a_2. \tag{28}$$

$$-\frac{a_{31}}{a_{11}}c_{11}(P_*,b_1^*)-\frac{a_{32}}{a_{22}}c_{21}(P_*,b_1^*)+c_{31}(P_*,b_1^*)\neq 0. \tag{29}$$

Proof. Consider the Jacobian matrix of the system (2) at $b_1=b_1^*$ can be written in the form:

$$M(P_*,b_1^*)=\begin{bmatrix}-d_1-a_1Y_* & 0 & -a_1C_*\\ 0 & -b_1^*X^* & X_*\left(\frac{-rh}{(1+hY_*)^2}-a_2+2b_2Y_*\right)\\ e_2a_1Y_* & Y_*\big(e_1(a_2-b_2Y_*)\big) & -e_1b_2X_*Y_*\end{bmatrix}=[a_{ij}],$$

where the characteristic equation given in Eq. (13), then for $b_1=b_1^*$, which is positive under condition (28), the value of $K=0$. Hence, it reduces to $\lambda[\lambda^2+A_1\lambda+A_2]=0$.

Therefore, there is a zero eigenvalue $\lambda_{*1}=0$, with the other two given by $\lambda_{*2},\lambda_{*3}=\frac{-A_1\pm\sqrt{A_1^2-4A_2}}{2}$.

Thus P_* is a nonhyperbolic equilibrium point for $b_1=b_1^*$. Now, to detect the occurrence of the saddle-node bifurcation, Sotomayer's theorem is applied.

Let $\boldsymbol{v}_*=(v_{41},v_{42},v_{43})^T$, and $\boldsymbol{\psi}_*=(\psi_{41},\psi_{42},\psi_{43})^T$ be the eigenvectors of $M(P_*,b_1^*)$, and $[M(P_*,b_1^*)]^T$ associated with $\lambda_{*1}=0$, then it obtain that $\boldsymbol{v}_*=\left(-\frac{a_{13}}{a_{11}},-\frac{a_{23}}{a_{22}},1\right)^T$, and $\boldsymbol{\psi}_*=$

$(-\frac{a_{31}}{a_{11}}, -\frac{a_{32}}{a_{22}}, 1)^T$.

Moreover, direct computation using Eq. (25) shows that:

$$\frac{\partial F}{\partial b_1} = F_{b_1} = (0, -X^2, 0)^T \;\Rightarrow\; \boldsymbol{\psi}_*{}^T[F_{b_1}(P_*, b_1^*)] = \frac{a_{32}}{a_{22}} X_*^2 \neq 0.$$

$$\boldsymbol{\psi}_*{}^T[D^2F(P_*, b_1^*)(\boldsymbol{v}_*, \boldsymbol{v}_*)] = -\frac{a_{31}}{a_{11}} c_{11}(P_*, b_1^*) - \frac{a_{32}}{a_{22}} c_{21}(P_*, b_1^*) + c_{31}(P_*, b_1^*).$$

Hence, under the condition (29) there is a saddle-node bifurcation in the sense of Sotomayor's theorem.

7. Numerical Simulation

An intensive numerical simulation of the system (2) is conducted in this section to gain a better understanding of the global dynamics of the proposed system, and specifically the control set of parameters. The Runge-Kutta of order four scheme was used to solve system (2) with the help of Matlab version R2021a, and then the obtained numerical results are drawn in the form of a 2D time series and a 3D phase picture using the following hypothetical set of parameters. Note that the red dot used in the following figures represents the equilibrium points, while the blue dot refers to different initial points.

$$\begin{array}{c} \Lambda = 2, d_1 = 0.1, a_1 = 0.2, r = 1, h = 0.2, d_2 = 0.15, \\ b_1 = 0.2, a_2 = 0.5, b_2 = 0.2, e_1 = 0.5, e_2 = 0.5, d_3 = 0.2 \end{array} . \tag{30}$$

As can be seen from Figure 1, the system (2) approaches asymptotically to the unique interior equilibrium point $P_* = (3.02, 3.31, 2.8)$ using the data set (30), starting from different initial values.

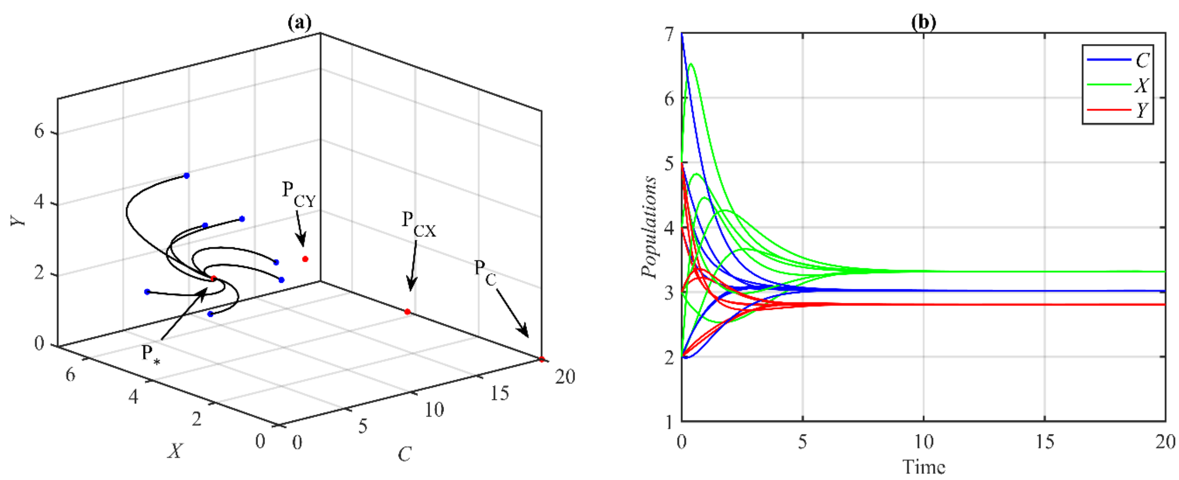

Fig. 1: The solutions of system (2) starting from different initial points using the data set (30). (a) All the solutions approach asymptotically to $P_* = (3.02, 3.31, 2.8)$. (b) The solutions as a function of time.

According to Figure 1, the system (2) has a globally stable interior equilibrium point, while the others are unstable.

Now, for the range $0 < b_2 \leq 0.09$, it is observed that the system approaches P_{CY}, while for $0.09 < b_2$, it approaches P_* as shown in Figure 2.

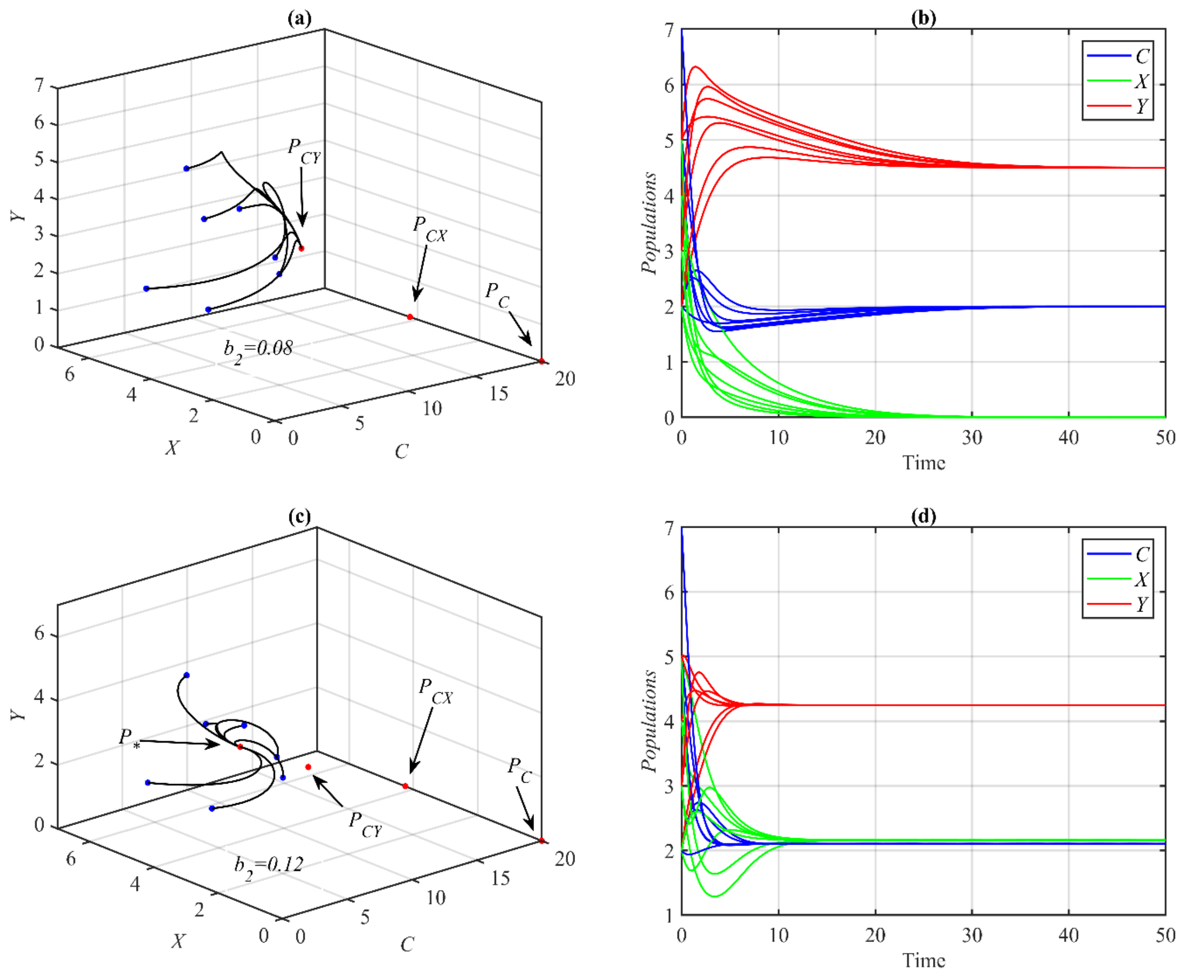

Fig. 2: The solutions of system (2) starting from different initial points using the data set (30). (a) All the solutions approach asymptotically to $P_{CY} = (2,0,4.5)$ when $b_2 = 0.08$. (b) The solutions as a function of time for $b_2 = 0.08$. (c) All the solutions approach asymptotically to $P_* = (2.1,2.16,4.24)$ when $b_2 = 0.12$. (d) The solutions as a function of time for $b_2 = 0.12$.

According to Figure 2, system (2) undergoes a bifurcation with bifurcation parameter b_2. It's observed that condition (11) is satisfied in the range $0 < b_2 \leq 0.09$, which leads to stability of P_{CY}, and otherwise it is violated.

Additionally, we observed that altering just one parameter results in a shift of the interior point's location without causing bifurcation. In contrast, confirming bifurcation in system (2) requires changing two or more parameters simultaneously. This occurs because the availability of carcasses as food, without the need for chasing, enhances the stability of the system at the interior point.

Now, for the data set (30) with $r = 0.1$ and $e_2 = 0.1$, it is observed that the system approaches asymptotically to $P_{CY} = (10,0,0.5)$ as the interior point disappears, and the condition (11) holds. However, for the data set (30) with $r = 0.1$, $e_2 = 0.1$, and $d_3 > 0.385$, all solutions of system (2) will approach $P_C = (20,0,0)$ due to the disappearance of all other equilibrium points, and condition (9) holds, see Figure 3.

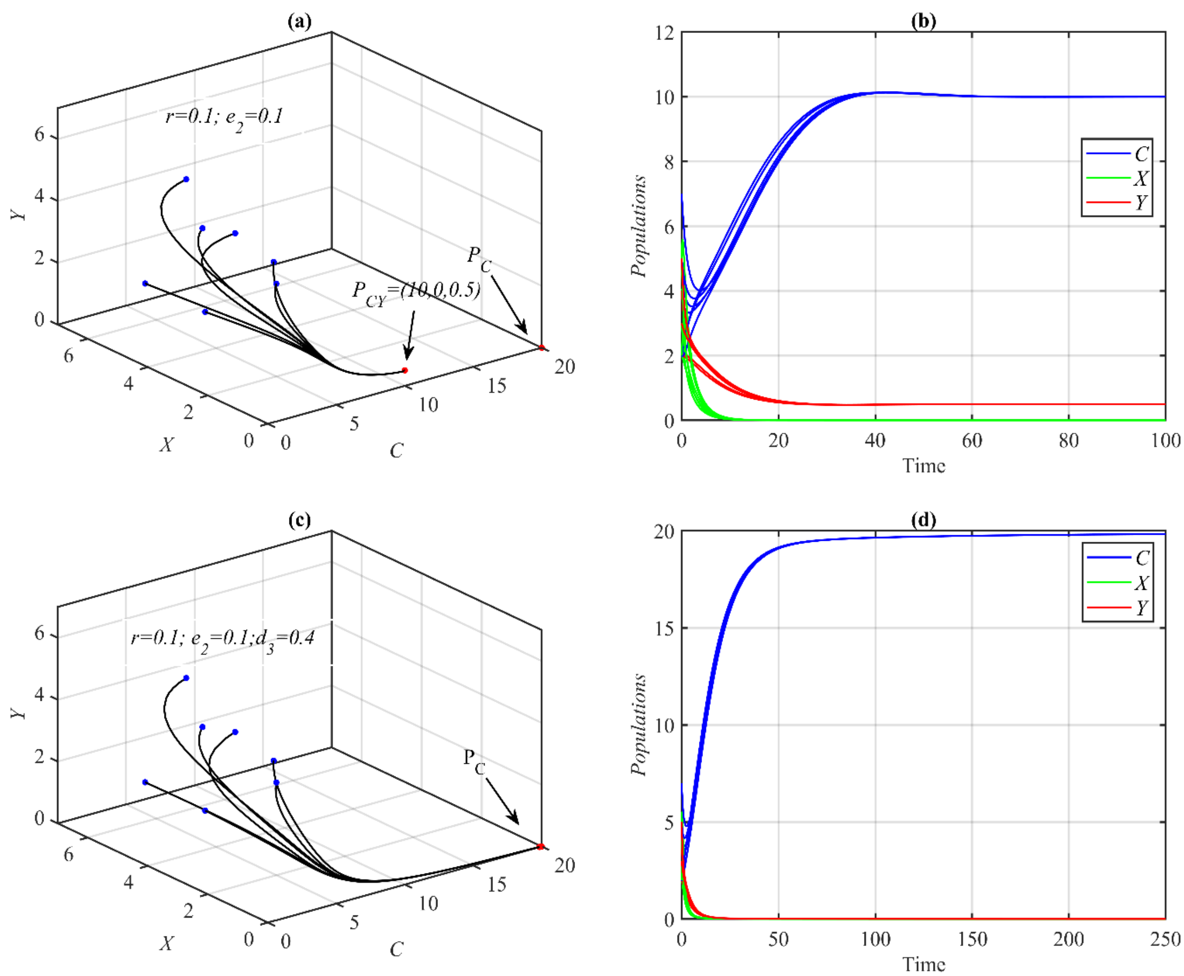

Fig. 3: The solutions of system (2) starting from different initial points using the data set (30). (a) All the solutions approach asymptotically to $P_{CY} = (10,0,0.5)$ when $r = 0.1$ and $e_2 = 0.1$. (b) The solutions as a function of time for $r = 0.1$ and $e_2 = 0.1$. (c) All the solutions approach asymptotically to $P_C = (20,0,0)$ when $r = 0.1$, $e_2 = 0.1$, and $d_3 = 0.4$. (d) The solutions as a function of time for $r = 0.1$, $e_2 = 0.1$, and $d_3 = 0.4$.

For the data set (30) with $e_1 = 0.1$, $e_2 = 0.1$, and $d_3 = 0.65$, it is observed that the system approaches asymptotically to $P_{CX} = (20,4.25,0)$ as the point P_{CY} and the interior point disappear, and the condition (10) holds, see Figure 4.

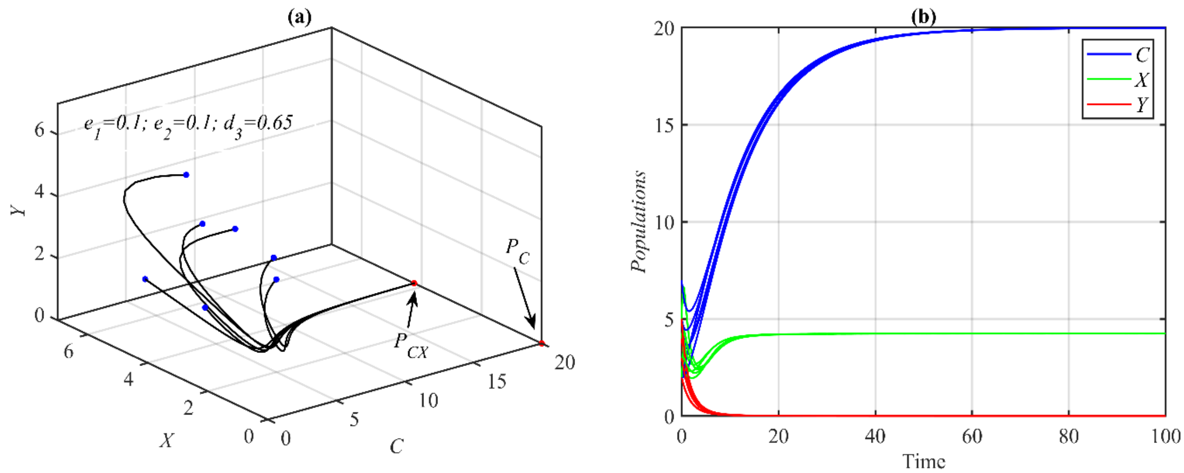

Fig. 4: The solutions of system (2) starting from different initial points using the data set (30). (a) All the solutions approach asymptotically to $P_{CX} = (20,4.25,0)$ when $e_1 = 0.1$, $e_2 = 0.1$, and $d_3 = 0.65$. (b) The solutions as a function of time for $e_1 = 0.1$, $e_2 = 0.1$, and $d_3 = 0.65$.

According to Figure 4, it is clear that when the conversion rates are reduced along with an increase in the scavenger's natural death rate, then the scavenger faces extinction and the system's solution approach to P_{CX}.

8. CONCLUSION

In this paper, the carcasses-prey-scavenger system was proposed and studied. It is obtained that there are at most four equilibrium points. All the requirements for their stability and persistence are determined. The conditions of occurrence of local bifurcation are established, too. It is obtained that the proposed system has only a point attractor, while periodic dynamics that naturally exist in a prey-predator system do not exist. This means the existence of carcasses in the environment stabilized the prey-predator dynamics. Moreover, although the numerical simulation confirms our obtained results, it refers to the following results.

The presence of carcasses in the environment has a stabilizing effect on the system by the disappearance of cyclic movement in the prey-predator system. The prey's net birth rate, the prey's and scavenger's natural death rate, the conversion rates, and the prey's refuge rate are the most effective parameters on the system dynamics.

CONFLICT OF INTERESTS

The authors declare that there is no conflict of interests.

REFERENCES

[1] É. Diz-Pita, M.V. Otero-Espinar, Predator–Prey Models: A Review of Some Recent Advances, Mathematics 9 (2021), 1783. https://doi.org/10.3390/math9151783.

[2] C.S. Holling, The Functional Response of Predators to Prey Density and Its Role in Mimicry and Population Regulation, Mem. Entomol. Soc. Can. 97 (1965), 5-60. https://doi.org/10.4039/entm9745fv.

[3] A.A. Berryman, The Orgins and Evolution of Predator‐Prey Theory, Ecology 73 (1992), 1530-1535. https://doi.org/10.2307/1940005.

[4] X. Wang, L. Zanette, X. Zou, Modelling the Fear Effect in Predator–Prey Interactions, J. Math. Biol. 73 (2016), 1179-1204. https://doi.org/10.1007/s00285-016-0989-1.

[5] S. Al-Momen, R.K. Naji, The Dynamics of Sokol-Howell Prey-Predator Model Involving Strong Allee Effect, Iraqi J. Sci. 62 (2021), 3114-3127. https://doi.org/10.24996/ijs.2021.62.9.27.

[6] A.R.M. Jamil, R.K. Naji, Modeling and Analysis of the Influence of Fear on the Harvested Modified Leslie–Gower Model Involving Nonlinear Prey Refuge, Mathematics 10 (2022), 2857. https://doi.org/10.3390/math10162857.

[7] A. Hastings, T. Powell, Chaos in a Three‐Species Food Chain, Ecology 72 (1991), 896-903. https://doi.org/10.2307/1940591.

[8] S.J. Majeed, R.K. Naji, A.A. Thirthar, The Dynamics of an Omnivore-Predator-Prey Model with Harvesting and Two Different Nonlinear Functional Responses, AIP Conf. Proc. 2096 (2019), 020008. https://doi.org/10.1063/1.5097805.

[9] H.A. Ibrahim, R.K. Naji, The Complex Dynamic in Three Species Food Webmodel Involving Stage Structure and Cannibalism, AIP Conf. Proc. 2292 (2020), 020006. https://doi.org/10.1063/5.0030510.

[10] P. Cong, M. Fan, X. Zou, Dynamics of a Three-Species Food Chain Model with Fear Effect, Commun. Nonlinear Sci. Numer. Simul. 99 (2021), 105809. https://doi.org/10.1016/j.cnsns.2021.105809.

[11] P. Panja, S. Gayen, T. Kar, D.K. Jana, Complex Dynamics of a Three Species Predator–Prey Model with Two Nonlinearly Competing Species, Results Control. Optim. 8 (2022), 100153. https://doi.org/10.1016/j.rico.2022.100153.

[12] F.H. Maghool, R.K. Naji, Chaos in the Three-Species Sokol-Howell Food Chain System with Fear, Commun. Math. Biol. Neurosci. 2022 (2022), 14. https://doi.org/10.28919/cmbn/7056.

[13] S. Pal, P.K. Tiwari, A.K. Misra, H. Wang, Fear Effect in a Three-Species Food Chain Model with Generalist Predator, Math. Biosci. Eng. 21 (2023), 1-33. https://doi.org/10.3934/mbe.2024001.

[14] B. Nolting, J.E. Paullet, J.P. Previte, Introducing a Scavenger onto a Predator-Prey Model, Appl. Math. E-Notes 8 (2008), 214–222.

[15] P. Panja, Prey–Predator–Scavenger Model with Monod–Haldane Type Functional Response, Rend. Circ. Mat. Palermo Ser. 2 69 (2019), 1205-1219. https://doi.org/10.1007/s12215-019-00462-9.

[16] H.A. Satar, R.K. Naji, Stability and Bifurcation in a Prey–Predator–Scavenger System with Michaelis–Menten Type of Harvesting Function, Differ. Equ. Dyn. Syst. 30 (2019), 933-956. https://doi.org/10.1007/s12591-018-00449-5.

[17] L.R. Ibrahim, D.K. Bahlool, Modeling and Analysis of a Prey-Predator-Scavenger System Encompassing Fear, Hunting Cooperation, and Harvesting, Iraqi J. Sci. 66 (2025), 2014-2037. https://doi.org/10.24996/ijs.2025.66.5.20.

[18] S.A. Rahi, R.K. Naji, The Role of Fear and Competition in the Dynamic of the Prey-Predator-Scavenger System, Ain Shams Eng. J. 16 (2025), 103494. https://doi.org/10.1016/j.asej.2025.103494.

[19] J.E. Jansen, R.A. Van Gorder, Dynamics from a Predator-Prey-Quarry-Resource-Scavenger Model, Theor. Ecol. 11 (2017), 19-38. https://doi.org/10.1007/s12080-017-0346-z.

[20] X. Wang, X. Zou, Modeling the Fear Effect in Predator–Prey Interactions with Adaptive Avoidance of Predators, Bull. Math. Biol. 79 (2017), 1325-1359. https://doi.org/10.1007/s11538-017-0287-0.

[21] R. Kumar Upadhyay, S. Mishra, Population Dynamic Consequences of Fearful Prey in a Spatiotemporal Predator-Prey System, Math. Biosci. Eng. 16 (2019), 338-372. https://doi.org/10.3934/mbe.2019017.

[22] P. Panday, N. Pal, S. Samanta, J. Chattopadhyay, Stability and Bifurcation Analysis of a Three-Species Food Chain Model with Fear, Int. J. Bifurc. Chaos 28 (2018), 1850009. https://doi.org/10.1142/s0218127418500098.

[23] H. Zhang, Y. Cai, S. Fu, W. Wang, Impact of the Fear Effect in a Prey-Predator Model Incorporating a Prey Refuge, Appl. Math. Comput. 356 (2019), 328-337. https://doi.org/10.1016/j.amc.2019.03.034.

[24] S. Samaddar, M. Dhar, P. Bhattacharya, Effect of Fear on Prey–Predator Dynamics: Exploring the Role of Prey Refuge and Additional Food, Chaos: Interdiscip. J. Nonlinear Sci. 30 (2020), 063129. https://doi.org/10.1063/5.0006968.

[25] F.H. Maghool, R.K. Naji, The Dynamics of a Tritrophic Leslie-Gower Food-Web System with the Effect of Fear, J. Appl. Math. 2021 (2021), 2112814. https://doi.org/10.1155/2021/2112814.

[26] S. Samaddar, M. Dhar, P. Bhattacharya, Effect of Fear on Prey–Predator Dynamics: Exploring the Role of Prey Refuge and Additional Food, Chaos: Interdiscip. J. Nonlinear Sci. 30 (2020), 063129. https://doi.org/10.1063/5.0006968.

[27] K. Parida, B.P. Sarangi, S. Chand, Impact of Fear and Anti-Predator Behavior on Stability and Chaos in Multi-Delayed Predator-Prey System, J. Appl. Math. Comput. 71 (2025), 8851-8886. https://doi.org/10.1007/s12190-025-02597-8.

[28] H.A. Ibrahim, D.K. Bahlool, H.A. Satar, R.K. Naji, Stability and Bifurcation of a Prey-Predator System Incorporating Fear and Refuge, Commun. Math. Biol. Neurosci. 2022 (2022), 32. https://doi.org/10.28919/cmbn/7260.

[29] F. Chen, On a Nonlinear Nonautonomous Predator–Prey Model with Diffusion and Distributed Delay, J. Comput. Appl. Math. 180 (2005), 33-49. https://doi.org/10.1016/j.cam.2004.10.001.

[30] L. Perko, Differential Equations and Dynamical Systems, Springer, (2001). https://doi.org/10.1007/978-1-4613-0003-8.

[31] T.C. Gard, Uniform Persistence in Multispecies Population Models, Math. Biosci. 85 (1987), 93-104. https://doi.org/10.1016/0025-5564(87)90101-5.